Herpes simplex virus type 1 infection in neurons leads to production and nuclear localization of APP intracellular domain (AICD): implications for Alzheimer's disease pathogenesis

Livia Civitelli[1,2] · Maria Elena Marcocci[1] · Ignacio Celestino[1] · Roberto Piacentini[3] ·
Enrico Garaci[4] · Claudio Grassi[3] · Giovanna De Chiara[5] · Anna Teresa Palamara[6]

Abstract Several data indicate that neuronal infection with herpes simplex virus type 1 (HSV-1) causes biochemical alterations reminiscent of Alzheimer's disease (AD) phenotype. They include accumulation of amyloid-β (Aβ), which originates from the cleavage of amyloid precursor protein (APP), and hyperphosphorylation of tau protein, which leads to neurofibrillary tangle deposition. HSV-1 infection triggers APP processing and drives the production of several fragments including APP intracellular domain (AICD) that exerts transactivating properties. Herein, we analyzed the production and intracellular localization of AICD following HSV-1 infection in neurons. We also checked whether AICD induced the transcription of two target genes, neprilysin (*nep*) and glycogen synthase kinase 3β (*gsk3*β), whose products play a role in Aβ clearance and tau phosphorylation, respectively. Our data indicate that HSV-1 led to the accumulation and nuclear translocation of AICD in neurons. Moreover, results from chromatin immunoprecipitation assay showed that AICD binds the promoter region of both *nep* and *gsk3*β. Time course analysis of NEP and GSK3β expression at both mRNA and protein levels demonstrated that they are differently modulated during infection. NEP expression and enzymatic activity were initially stimulated but, with the progression of infection, they were down-regulated. In contrast, GSK3β expression remained nearly unchanged, but the analysis of its phosphorylation suggests that it was inactivated only at later stages of HSV-1 infection. Thus, our data demonstrate that HSV-1 infection induces early upstream events in the cell that may eventually lead to Aβ deposition and tau hyperphosphorylation and further suggest HSV-1 as a possible risk factor for AD.

Keywords Alzheimer's disease · Herpes simplex virus (HSV-1) · APP · Neurodegeneration · AICD · Neprilysin · GSK3β

Livia Civitelli and Maria Elena Marcocci contributed equally to this work.

✉ Livia Civitelli
livia.civitelli@liu.se

[1] Department of Public Health and Infectious Diseases, Sapienza University of Rome, Rome, Italy

[2] Experimental Pathology, Department of Clinical and Experimental Medicine, Linköping University, Linköping, Sweden

[3] Institute of Human Physiology, Università Cattolica del Sacro Cuore, Rome, Italy

[4] IRCCS San Raffaele Pisana, Telematic University, Rome, Italy

[5] Institute of Translational Pharmacology, CNR, Rome, Italy

[6] Department of Public Health and Infectious Diseases, Institute Pasteur Cenci Bolognetti Foundation, Sapienza University of Rome, Rome, Italy

Introduction

Alzheimer's disease (AD) is a neurodegenerative disorder, mainly constituted by progressive neuronal death, brain atrophy, and cognitive impairment. The major pathological hallmarks of AD include extraneuronal deposits of the amyloid-β peptide (Aβ) and intraneuronal accumulation of hyperphosphorylated microtubule-associated tau protein, which forms neurofibrillary tangles (NFTs) (Masters and Selkoe 2012). Aβ is physiologically produced by a processing of the amyloid precursor protein (APP) (the so-called amyloidogenic processing), which begins when this integral membrane protein undergoes cleavage by the β-secretase (BACE1), giving rise to the release of the N-terminal soluble

fragment (sAPPβ) (Haass et al. 2012). Then, γ-secretase catalyzes the intramembrane proteolysis of the APP C-terminal portion (CTFβ) to produce different fragments including Aβ, APP intracellular domain (AICD), and p3 (Zhang et al. 2011). The role of AICD is an open question, but it has been proposed to have a transactivation activity (Słomnicki and Leśniak 2008; Cao and Südhof 2001), regulating the transcription of multiple genes, whose protein products potentially concur to the neurodegeneration. Several indication points to the aggregation and accumulation of Aβ within the brain in sporadic AD patients may be due either to an impairment of the Aβ clearance system or to deficiencies in the enzyme-mediated Aβ degradation rather than to an increase in Aβ production (references in Nixon 2007). Many proteases have been described to degrade endogenous Aβ, among other neprilysin (NEP), a zinc-dependent metalloprotease involved in the maintenance of Aβ homeostasis in the brain together with other enzymes (Wang et al. 2010).

Epidemiological data suggest that herpes simplex virus type 1 (HSV-1) is one of the environmental risk factors for AD (Piacentini et al. 2014; De Chiara et al. 2012). HSV-1 is very common human pathogens, which infects between 40 and 80 % of people worldwide (Xu et al. 2006). It commonly causes infection in the orofacial region, but it can also be responsible of keratitis, genital herpes, and encephalitis. HSV-1 generally causes latent infections in the nervous ganglia that are reached by the virus through axonal retrograde transport. Latent virus reactivates periodically so that newly formed HSV-1 virions return to the initial infection site, causing recurrent infections (Mori et al. 2004; Dobson and Itzhaki 1999). HSV-1 may also reach the brain, targeting the same regions altered in AD, where it may establish latent infections and reactivate periodically. In the brain of AD patients, viral DNA was found associated with senile plaques, and different groups demonstrated the involvement of HSV-1 infection in Aβ production in neuronal cells (Santana et al. 2012; Piacentini et al. 2011, De Chiara et al. 2010; Wozniak et al. 2007). Our previous data demonstrated that HSV-1 induces the amyloidogenic processing of APP in neuronal cells, causing the formation of multiple APP neurotoxic fragments (De Chiara et al. 2010), including Aβ oligomers and CTFs. In addition, HSV-1 infection is associated to AD-related hyperphosphorylation of tau (Lerchundi et al. 2011; Zambrano et al. 2008), possibly through the action of glycogen synthase 3β (GSK3β) (Wozniak et al. 2009), a serine/threonine kinase, whose activation is regulated by phosphorylation at different sites.

Here, we focused on the effects of HSV-1 infection on the production and biological activity of CTF-derived AICD fragment. We demonstrate that during HSV-1 infection, both CTFs and AICD accumulated within the nucleus of infected cells, and that AICD directly bound to the promoter region of both *nep* and *gsk3*β genes. We also found that HSV-1

infection modulated the transcription and expression of NEP, as well as its enzymatic activity, throughout the infection. On the contrary, GSK3β expression level remained nearly stable during infection, and its activation lasted until the later stages of infection.

Materials and methods

Ethics statement

The procedures regarding animals were approved by the Ethics Committee of the Catholic University, in agreement with Italian Ministry of Health guidelines, with national laws (Legislative decree 116/1992) and European Union guidelines on animal research (No. 86/609/EEC).

Reagents and antibodies

Rabbit polyclonal antibodies against GSK3β (clone 27C10), p-Ser9-GSK3β, APP, IgG were purchased from Cell Signaling Technology, whereas mouse monoclonal anti-NEP (H-321) and anti-APP 643–695 (MAB343) antibodies from Santa Cruz Biotechnology and Chemicon, respectively. Mouse monoclonal anti-Tubulin was purchased from Sigma. Goat polyclonal anti-HSV-1 antibody was purchased from AbD Serotec. Thiorphan (DL) and captopril were purchase from Santa Cruz Biotechnology, Mca-R-P-P-G-F-S-A-F-K(Dnp)-OH Fluorogenic Peptide Substrate was obtained from R&D Systems, and 1,10-Phenanthroline was purchased from Aldrich.

Virus production and titration

Monolayers of VERO cells were cultivated in 75 cm^2 tissue culture flasks and infected with HSV-1 strain F at a multiplicity of infection (m.o.i.) of 0.01 as previously described (De Chiara et al. 2010). After 48 h at 37 °C, infected cells were collected and went through 3 cycles of freeze-and-thaw. Cell debris was removed with low-speed centrifugation, and virus titers were measured by standard plaque assay (Killington and Powell 1991). In this study, the virus had a titer of 5×10^8 plaque forming units (pfu)/ml. The virus was stored at −80 °C until used.

Cell cultures and HSV-1 infection

Primary cultures of cortical neurons were prepared from E18-E19 Wistar rat embryos as previously described (Piacentini et al. 2011). In brief, cortices were dissected and incubated for 10 min at 37 °C in phosphate buffer saline (PBS) containing trypsin-ethylenediaminetetraacetic acid (0.025 %/0.01 % *w*/*v*; Biochrom AG). The tissue was tritured at room

temperature (RT) with a Pasteur pipette. The cell suspension was centrifuged at 235×g for 8 min. The pellet was resuspended in 88.8 % Minimum Essential Medium (Biochrom), 5 % fetal bovine serum (FBS, Invitrogen), 5 % horse serum, 1 % glutamine (2 mM), 1 % penicillin-streptomycin-neomycin antibiotic mixture (Invitrogen), and glucose (25 mM) and cells plated on pre-coated poly-L-lysine (Sigma) round coverslips (density, 4×10^4 to 1×10^5 cells/coverslip). The following day, the medium was replaced with a mixture of 96.5 % Neurobasal medium (Invitrogen), 2 % B-27 (Invitrogen), 0.5 % glutamine (2 mM), and 1 % penicillin-streptomycin-neomycin antibiotic mixture. After 72 h, a glutamine-free version of the medium was added to the cells that were grown for ten more days prior to experiments. SH-SY5Y neuroblastoma cells were cultivated as already described (De Chiara et al. 2010). Briefly, they were grown in Dulbecco's modified Eagle's medium (DMEM; Biochrom) containing 15 % heat-inactivated FBS and antibiotics (glutamine 0.3 mg/ml, penicillin 100 units/ml, streptomycin 100 μg/ml) and then plated on round coverslips. For experiments, cells were challenged with wild-type HSV-1 (m.o.i 1) for 1 h at 37 °C, washed with PBS, and incubated with medium supplemented with 2 % FBS (or returned to the original medium in the case of rat cortical neurons). Mock-infection was performed with conditioned medium from uninfected VERO cells by using the same dilution as that used for the virus. Virus production was assessed by standard plaque assay of cell supernatants collected at different times post infection (p.i.).

Chromatin immunoprecipitation

ChIP assays were performed as previously described (Weinmann and Farnham, 2002). Briefly, ~5×10^6 cells were used, and at the different time p.i., formaldehyde (1 %) was added directly to the medium for 10 min. After stopping the cross-linking reaction with 0.2 M glycine, cells were harvested by centrifugation. Pellets were resuspended in 200 μL lysis buffer (1 % SDS, 50 mM Tris–HCl pH 8.1, 10 mM EDTA). Then, samples were sonicated on ice with duty 50 %, 0.5″ on/off, 2 cycles 40″, 6 cycles 20″. Following centrifugation to remove cell debris, supernatants were pre-cleared by incubation with protein-G Sepharose 4B beads (Sigma-Aldrich) for 1 h at 4 °C. Beads were removed by centrifugation, and supernatants were subjected to immunoprecipitation. A fraction of the supernatant was subsequently used as the total input control; 1–3 μg of the AICD specific antibody (BR188, a kindly gift from Dr M. Goedert, Cambridge, UK; Lefranc-Jullien et al. 2006) or rabbit IgG was added overnight at 4 °C on a rotating platform. Immune complexes were incubated with protein-G Sepharose 4B beads for 2 h at 4 °C, then subjected to a series of eight sequential washes, with law-salt buffer (0.1 % SDS, 1 % Triton X-100, 2 mM EDTA pH 8,

20 mM Tris-HCl pH 8, 150 mM NaCl), high-salt buffer (0.1 % SDS, 1 % Triton X-100, 2 mM EDTA pH 8, 20 mM Tris-HCl pH 8, 500 mM NaCl), lithium buffer (10 mM Tris HCl pH 8, 1 mM EDTA pH 8, 0.1 % deoxycholate, 1 % NP40, 250 mM LiCl), and 1× TE (pH 8). Immune complexes were eluted with a buffer containing SDS (1 %) and NaHCO$_3$ (pH 8.0, 0.1 M) for 15′ with rotation. The cross-linking reaction was performed by adding NaCl 0.2 M followed by incubation at 65 °C overnight. DNA fragments were purified by using the QIAquick PCR Purification Kit (Qiagen) and analyzed in real-time PCR to quantify changes in AICD promoter occupancy in infected- versus mock-infected cells. Specific sets of primers flanking promoter region of nep (Belyaev et al. 2009) and gsk3β genes (PromGsk3β_F: ACGCCCTCCC TTCGCTTTC; PromGsk3β_R: GGCTTCCGAGGACAGT CTGG) were designed. PCR conditions and cycle numbers were empirically set for the different templates and primer pairs. PCR conditions are available on request. Real-time PCR was run in an iCycler IQ5 (Biorad) with the IQ™ SYBR Green Supermix (Biorad) reagent. Real-time PCR results are represented as fold enrichment of DNA pulled down with BR188 over the enriched DNA from IgG.

Real-time PCR

Real time experiments were performed as described elsewhere (De Chiara et al. 2010). Total RNA was obtained from mock- and HSV-1-infected cortical neurons collected at the indicated times p.i. with the RNeasy Kit (Qiagen) and quantified by ultraviolet spectrometry at 260 nm. The iScript™ cDNA Synthesis Kit (Biorad) was used to perform the reverse-transcription of 1 μg of RNA. Relative quantitative real-time PCR was performed with the IQ™ SYBR Green Supermix (Biorad) reagent. Fluorescein was included in each reaction for well-factor collection. All PCR reactions were coupled to melting-curve analysis to confirm the specificity of the products. The PCR was set with a denaturation step at 95 °C for 3 min, then 40 cycles at 95 °C for 10 s and at 58 °C for 30 s. The rRNA 18S was used to quantify each PCR product. The relative quantification was calculated with iCycler IQ5 analysis software. Specific sets of primers were designed as described in Table 1.

Western blot analysis

Western blot experiments were performed as already described (De Chiara et al. 2010). Briefly, cell pellet was resuspended in cold lysis buffer (10 mM Tris-HCl, 150 mM NaCl, 1 mM phenylmethylsulfonyl fluoride (PMSF), phosphatase inhibitor mixture [Sigma], and 1 % Triton X-100, pH 7.4), and incubated for 30 min on ice. After centrifugation (13000×g for 30 min), the supernatants were collected and the protein concentration was determined (Bradford method,

Table 1 Primers used for real-time PCR analysis

18S_F	5′-GTAACCCGTTGAACCCCATT-3′
18S_R	5′-CCATCCAATCGGTAGTAGCG-3′
GAPDH_F	5′-TGCACCACCAACTGCTTAGC-3′
GAPDH_R	5′-GGCATGGACTCTGGTCATGAG-3′
GSK3β_F	5′-ACCGCAGAACCTCTTGTTGGATC-3′
GSK3β_R	5′-ACACAGCCAGCAGACCATACATC-3′
NEP_F	5′- AAGATGGAGCCTCGTTGACTGG-3′
NEP_R	5′-TCTGATAGGCTCTGTATGCTTGGC-3′

Bio-Rad). Same amount of proteins was resuspended in SDS buffer with 100 mM DTT, separated with SDS-PAGE, and blotted onto nitrocellulose membranes for western blot analysis. The membranes were blocked with 10 % nonfat dry milk in TBS-Tween 0.1% for 1 h at RT. Primary antibodies were added at a final concentration of 1 μg/ml. Secondary antibodies were horseradish peroxidase-conjugated (Jackson ImmunoResearch). Western blot membranes were developed with the Pierce ECL Plus Western Blotting Substrate (Thermo Scientific) and subjected to densitometric scanning. For additional incubation, membranes were stripped by using the Restore™ Western Blot Stripping Buffer (Thermo Scientific).

Fractionation studies

Fractionation studies were performed mainly as already described (Lesné et al. 2006). Briefly, after the isolation of the cytoplasmic fraction, membrane-associated proteins were extracted by adding 50 mM Tris-HCl (pH 7.4), 150 mM NaCl, 0.5 % Triton X-100, 1 mM EGTA, 3 % SDS, 1 % deoxycholate, 1 mM PMSF, and protease inhibitor cocktail (Sigma-Aldrich) to the pellet of infected- or mock-infected cortical neurons. After 30′ incubation on a rotating platform, the samples were centrifuged for 90′ at 14,000×g at 4 °C. The supernatant was collected and protein concentrations were obtained with BCA Protein Assay kit (Pierce). Equal amounts of proteins from infected- and mock-infected protein extracts were incubated with MAB343 antibody (1 μg/ml) overnight at 4 °C to immunoprecipitate APP C-terminal fragments. Immunoprecipitates were separated by 15 % SDS-PAGE gel, blotted onto 0.22 μm nitrocellulose membrane and stained with BR188 antibody. Blots were developed as described above.

Immunoprecipitation studies

Immunoprecipitation studies were performed as already described (De Chiara et al. 2010). Nuclear and cytoplasmic proteins from infected- and mock-infected cortical neurons were obtained with the NE-PER Nuclear and Cytoplasmic Extraction kit (Pierce). The protein concentrations were assessed with BCA Protein Assay kit (Pierce). Equal amounts of

nuclear and cytoplasmic proteins were incubated with MAB343 antibody (1 μg/ml) overnight at 4 °C and analyzed as described above.

Enzymatic protein assay

Cellular lysates from mock- and HSV-1-infected rat cortical neurons were used to evaluate NEP activity through a fluorogenic enzyme assay. Briefly, equal amounts of cellular lysates (100 μg) were incubated in 50 mM Tris HCl, pH 7.4 with 1 μM captopril for 10′ on ice and then treated with or without 2 mM thiorphan (a specific inhibitor of NEP activity) for 25′ at room temperature. The mixture was charged with the Mca-R-P-P-G-F-S-A-F-K (Dnp)-OH Fluorogenic Peptide Substrate (10 μM) and incubated in the dark for 1 h at 37 °C. The reaction was stopped at 100 °C for 5′, then the samples were centrifuged at 2500×g for 5′. The samples were diluted 1:2 with 50 mM Tris HCl, pH 7.4 and loaded on 96-well plates to measure the fluorescence in a fluorescent plate reader (Perkin Elmer LS50B, excitation at 320 nm and emission at 405 nm). The amount of fluorescent product generated by NEP activity was determined by subtracting the arbitrary fluorescence units produced by samples incubated with thiorphan from the arbitrary fluorescence units produced by samples incubated without thiorphan.

Immunocytochemistry

Cortical neurons and SH-SY5Y cells were treated for immunocytochemistry as described previously (Piacentini et al. 2011). Briefly, cells were fixed with 4 % paraformaldehyde (Sigma) in PBS for 15 min at RT, permeabilized with 0.3 % Triton X-100 (Sigma) in PBS for 15 min, and then blocked with 0.3 % bovine serum albumin (in PBS) for 20 min. Cells were then incubated overnight at 4 °C with the following antibodies: mouse anti-MAP2 (1:500, Sigma); goat anti-HSV-1 (1:500; Millipore); and rabbit anti-AICD (1:500; Signet-Covance, Princeton, New Jersey). The following day, cells were incubated for 90 min at RT with a mixture of the following secondary antibodies: goat anti-rabbit Alexa Fluor 488 (1:1000; Invitrogen); donkey anti-goat Alexa Fluor 633 (1:1000; Invitrogen); and donkey anti-mouse Alexa Fluor 546 (1:1000; Invitrogen). Nuclei were then counterstained with 4′,6-diamidino-2-phenylindole (DAPI, 0.5 μg/ml for 10 min; Invitrogen), and the cells were coverslipped with Pro-Long Gold anti-fade reagent (Invitrogen). Images (512× 512 pixels) from at least 10 random 63× fields were obtained with a confocal laser scanning system (TCS-SP2, Leica Microsystem, Wetzlar, Germany). An Ar/ArKr laser and two HeNe lasers were used for 488, 543, and 633 nm excitation, respectively, and an ultrafast, tunable, mode-locked titanium:sapphire laser (Chamaleon, Coherent Inc., Santa Clara, CA) for two-photon excitation of fluorophores.

Quantitative analysis of AICD immunoreactivity was performed by quantifying the mean fluorescence intensity in a region of interest traced around cell nuclei. For cortical neurons, analysis was limited only to cells clearly positive to MAP2 staining. Control experiments in which cells were incubated with the secondary antibodies alone were carried out and no unspecific labeling was observed (data not shown). The specificity of AICD labeling was verified by evaluating the AICD immunoreactivity in cultures treated with InSolution® γ-secretase inhibitor X (10 μM; Calbiochem, Merck, KGaA, Darmstad, Germany).

Statistical analyses

Statistics were calculated by using Student's *t* test or two-way ANOVA when appropriate. Threshold for significance was set at $p<0.05$. Data are presented as means±S.D.

Results

HSV-1-induced APP amyloidogenic processing leads to AICD production and nuclear localization

In a first set of experiments, we studied production and intracellular localization of CTFs in rat cortical neurons challenged with HSV-1 (at 1 m.o.i.) or mock-infected. Cells were collected either 1 h after virus challenge, i.e., soon after virus adsorption (post challenge, p.c.) or 18 h post infection (p.i.), and membrane-enriched fractions were immunoprecipitated with anti-APP C-terminal antibody. As shown in Fig. 1a (left panel), in HSV-1 infected cells, CTFs were mostly found in the membranes 1 h p.c., but not 18 h p.i.. We then checked whether these results reflected the nuclear translocation of CTFs and/or their further cleavage in HSV-1-infected cells. Western blot analysis on subcellular fractions revealed that 18 h p.i. CTFs were more abundant in nuclear compartment of virus infected-cells than in mock-infected ones (Fig. 1a, right panel). Immunofluorescence analysis allowed us to explore the further cleavage of CTFs and the formation of AICD in HSV-1-infected cells. Both human neuroblastoma SH-SY5Y cells and rat cortical neurons were infected with HSV-1 and stained with anti-AICD antibody at different time points p.i.. In SH-SY5Y cells, intranuclear AICD levels raised with the progression of infection (Fig. 1b–e), whereas in rat cortical neurons, the peak of AICD intranuclear accumulation was found at 15 h p.i. (Fig. 1f–i). Staining with HSV-1 antibody revealed that AICD accumulated in infected cells, and the different intensity in their staining indicated various stages of viral replication

within cells, since the antibody used was raised against both early and late viral proteins (Fig. 1j).

As shown in Fig. 1l (bar graph on the left), the mean nuclear immunoreactivity for AICD was greater in HSV-1-infected than in mock-infected cells: in SH-SY5Y neuroblastoma cells increases of +154, +163, and +211 % were found at 12, 15, and 18 h p.i., respectively ($p<0.0001$); in rat cortical neurons, they were +29, +78, and +45 %, respectively, at the same time points; $p<0.0001$.

In rat cortical neuron cultures, only cells exhibiting the morphological features of mature neurons were taken into consideration and analyzed, as shown by anti-Map2 antibody staining (Fig. 1k). Since AICD production is catalyzed by γ-secretase, which cuts APP in the C-terminal domain, we performed control experiments infecting cells in the presence of the specific γ-secretase inhibitor X. Under these experimental conditions, HSV-1 infection failed to significantly increase AICD production (Fig. 1l–o). Our data indicate that HSV-1 infection increases the production of AICD, which accumulates in the nucleus of HSV-1-infected neuronal cells.

AICD produced during HSV-1 infection binds the promoter region of gsk3β and nep genes and increases their transcription

To delve into the molecular function of AICD as a regulator of *gsk3*β and *nep* expression, we checked whether, during HSV-1 infection, it interacted directly with the promoter region of these genes. Rat primary cortical neurons were infected with HSV-1, and cells were subjected to ChIP assay. AICD binding to the region of *gsk3*β and *nep* promoters was determined by real-time PCR. Since the expression of the *nep* gene may be under the control of two distinct promoters, identified as NEP*prom*1 and NEP*prom*2 (Li et al. 1995), we investigated AICD binding to both. As shown in Fig. 2a, in HSV-1-infected cells, AICD bound to both NEP*prom*1 and NEP*prom*2 and *gsk3*β promoter (GSK3β*prom*) mainly 15 h p.i.. Control experiments demonstrated that the increased binding of AICD to the promoters of *nep* and *gsk3*β was abolished when cells were grown in the presence of the γ-secretase inhibitor (Fig. 2b). We then decided to analyze *gsk3*β and *nep* transcript levels during HSV-1 infection. Rat cortical neurons were infected; cells were collected 12, 15, and 18 h p.i.; and mRNA levels were analyzed for both genes. We found that *nep* mRNA levels progressively increased starting from 12 h p.i, reaching a peak 15 h p.i., and decreasing 18 h p.i.. On the contrary, the level of *gsk3*β mRNA was more stable as no statistically significant differences were found at any time p.i. (Fig. 3). These data suggest that the two genes respond in different way to the presence of AICD at the promoter region during viral infections.
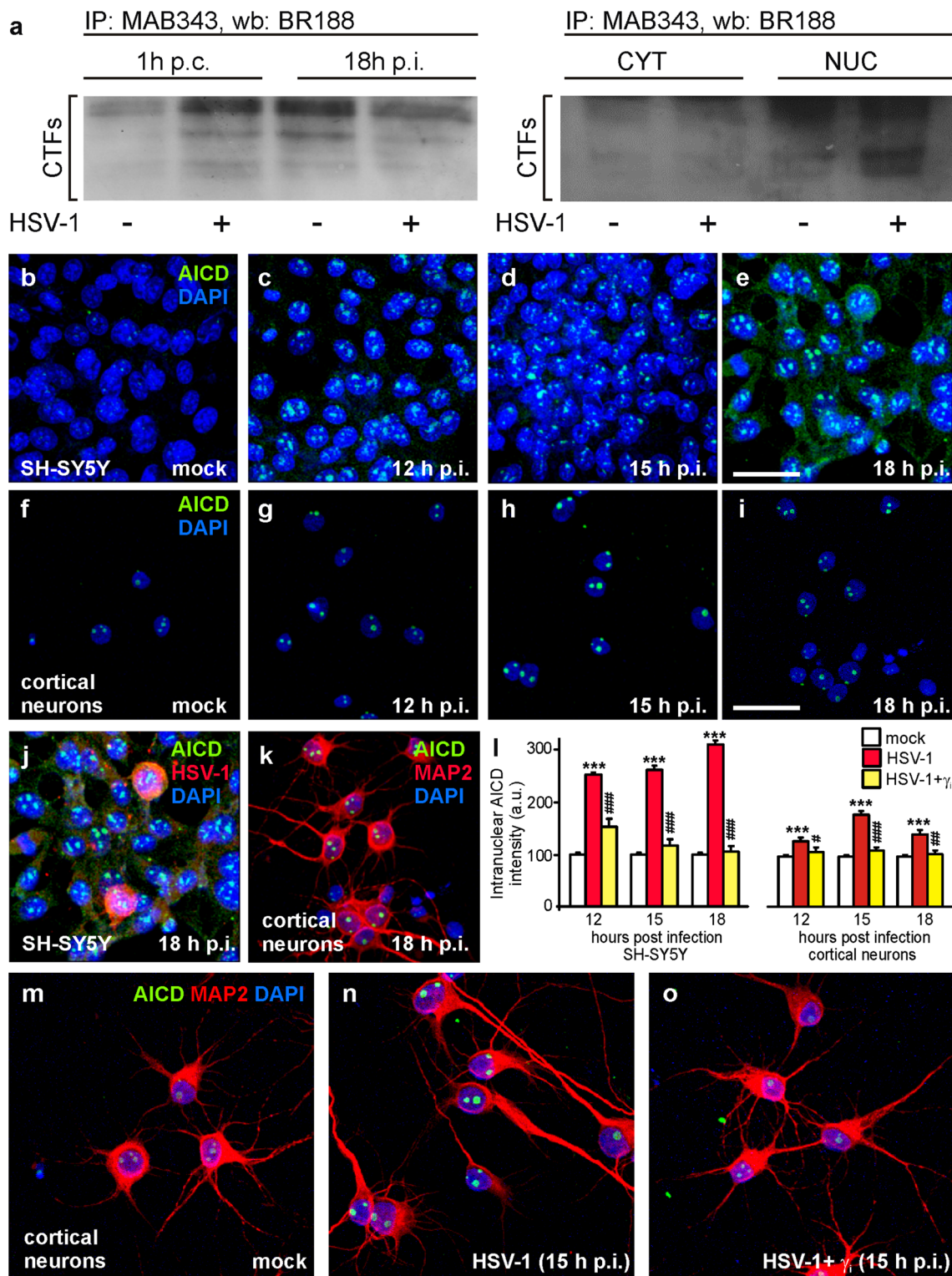
NEP expression and its enzymatic activity are modulated during HSV-1 infection

Then, we evaluated whether the expression and the enzymatic activity of the related protein (NEP) mirrored the

AICD-induced modulation of *nep* mRNA levels. As shown in Fig. 4a, viral infection induced an increase in the expression of NEP 15 h p.i. ($p<0.05$ vs mock-infected cells), followed by its decrease with the progression of the infection ($p<0.001$ 18 h p.i. vs mock infected cell). NEP

◀ **Fig. 1** HSV-1 infection induces AICD formation and its nuclear localization in host cells. **a** Membrane-enriched fractions from mock- or HSV-1-infected rat cortical neurons immunoprecipitated with anti-APP C-terminal antibody (MAB 343) at 1 h after virus challenge (p.c.) and 18 h p.i., and revealed by BR188 antibody (*left panel*). CTFs from cytoplasmic and nuclear compartment of mock- and HSV-1-infected cells isolated 18 h p.i. were immunoprecipitated with MAB 343 and revealed by BR188 antibody (*right panel*). **b–k** Confocal microscopic images of mock- or HSV-1-infected SH-SY5Y cells and rat cortical neurons at the indicated time points p.i.. Cells were labeled with anti-AICD, anti-Map2, or anti-HSV-1 antibodies, and nuclei were stained with DAPI. The color of the fluorescence representing each primary antibody is indicated. **l** *Bar graphs* showing mean intranuclear AICD fluorescence intensity in the condition presented in panels **b–e** for SH-SY5Y cells and **f-i** for cortical neurons. ***$p < 0.0001$ vs. mock; #$p < 0.05$ vs HSV-1; ##$p < 0.001$ vs HSV-1; ###$p < 0.0001$ vs HSV-1. **m–o** Confocal microscopic images of rat cortical neurons infected in the presence of the specific γ-secretase inhibitor X. All results are shown for one representative experiment of three performed. *Scale bars*, 50 μm

enzymatic activity is also increased 15 h p.i., but then, it decreased, exactly as the protein expression level (Fig. 4b).
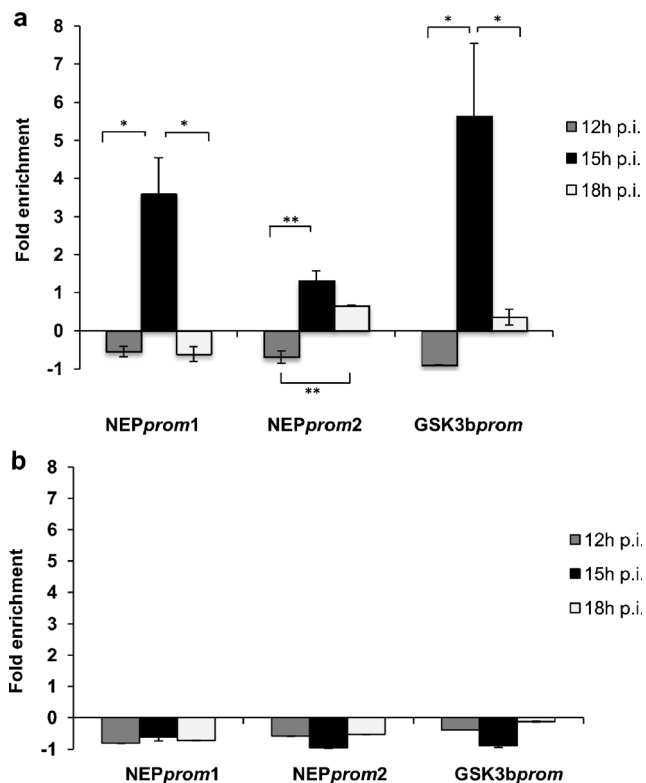

Fig. 2 AICD produced during HSV-1 infection binds *nep* and *gsk3*β promoters. **a** Rat cortical neurons were infected with HSV-1 and, at the indicated times p.i., subjected to ChIP assay with BR188 antibody, or, as control, with anti-IgG antibody. Changes in AICD occupancy at the promoters of *nep* (NEP*prom*1, NEP*prom*2) and *gsk3*β (GSK3β*prom*) genes were quantified by real-time PCR. Data are shown as the fold enrichment of DNA pulled down with BR188 relative to DNA pulled down with IgG in infected- versus mock-infected cells. Data are expressed as means±S.D. of three independent experiments, *$p < 0.05$, **$p < 0.01$. **b** ChIP assay of HSV-1- or mock-infected rat cortical neurons at the indicated times p.i., treated with the γ-secretase inhibitor X. Data are expressed as means±S.D. of three independent experiments
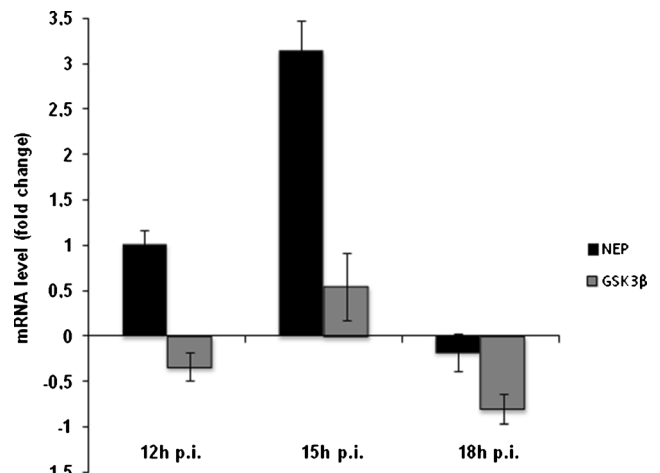

Fig. 3 *nep* and *gsk3*β transcripts increase during HSV-1 infection. Rat cortical neurons were infected with HSV-1 and NEP and GSK3β mRNA levels were analyzed at the indicated time p.i. by using real-time PCR. mRNA levels are expressed as fold change versus mock-infected cells. Results are means±S.D. for one representative experiment of four performed, each run in triplicate

These results indicate that NEP expression and its enzymatic activity are modulated during HSV-1 infection.

HSV-1 does not modulate GSK3β protein expression level

Previous studies showed that HSV-1 infection leads to GSK3β activation that, in turn, phosphorylates microtubule-associated protein tau at specific sites (Wozniak et al. 2009). Therefore, even though *gsk3*β mRNA levels appeared stable during viral infection (Fig. 3), we decided to analyze the effect of the virus on GSK3β expression and phosphorylation status, and particularly the phosphorylation at serine 9 (Ser9), which is known to be associated with inactivation of GSK3β activity (Medina and Wandosell 2011). Samples from HSV-1- and mock-infected cells were analyzed in western blot 12, 15, and 18 h p.i.. We found that the total level of GSK3β did not significantly change along the progression of the infection (Fig. 5). Moreover, Ser9 phosphorylation increased in infected cells only at later stages of viral infection, reaching statistical significance 15 and 18 h p.i. ($p < 0.05$). These results indicate that GSK3β is phosphorylated in Ser 9 in the late stages of viral infection (Fig. 5a and c), and suggests that the protein is active at earlier times p.i..

Discussion

In our study, we demonstrate that HSV-1 increased the production and intranuclear localization of C-terminal products derived from APP amyloidogenic cleavage: CTFs and AICD. With regard to CTFs, here, we show that they have a different intracellular localization during viral infection. In fact, 18 h

Fig. 4 HSV-1 infection modulates NEP protein expression and its enzymatic activity. **a** Representative blot of lysates from mock- and HSV-1-infected rat cortical neurons collected at the indicated time points p.i., immunostained with anti-NEP antibody, and with anti-Tubulin antibody as loading control. Densitometric analysis of NEP levels on immunoblots from four different experiments is shown in the graph (*right panel*); *$p<0.05$, ***$p<0.001$ HSV-1 vs mock. **b** Fold changes in NEP activity measured with enzymatic fluorimetric assay and compared to mock. For each sample, two fluorimetric readings were averaged. Results are means± S.D. of four independent experiments (HSV-1 vs mock, **$p<0.01$)
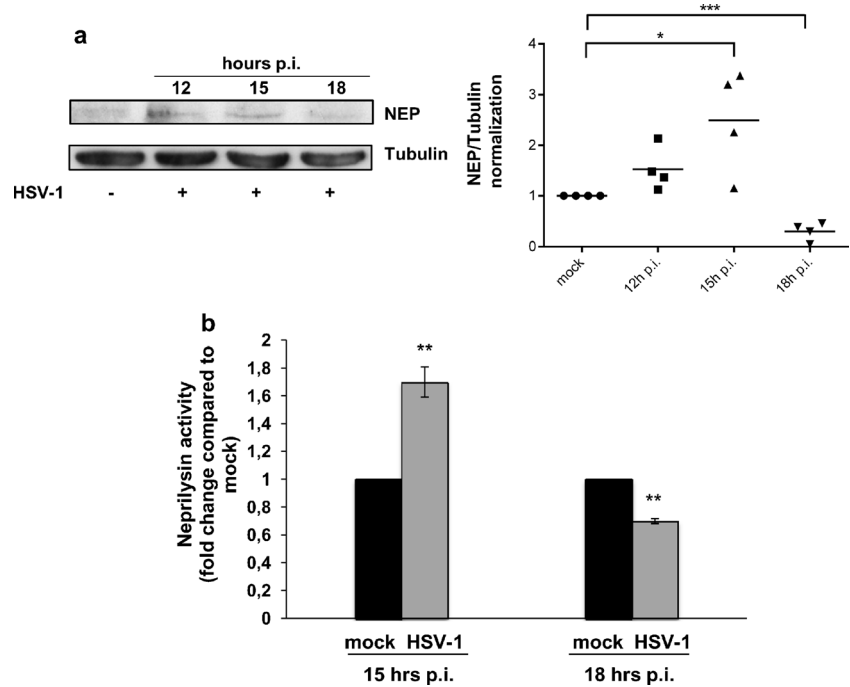
p.i. in infected cells, a small amount of CTFs are present in the membranes as compared with mock-infected ones, whereas they appear accumulated in the nucleus at the same time p.i. The observed decrease in membrane-bound CTFs could result from the HSV-1-induced shut down of host protein synthesis affecting APP (De Chiara et al. 2010; Shipley et al. 2005). Otherwise, it could reflect a substantial increase of their further cleavage by γ-secretase to produce AICD. Interestingly, a significant decrease of CTFs in specific brain areas of AD patients (temporal and occipital cortex) was demonstrated by Sergeant et al. (2002), suggesting that the fate of CTFs could mirror the progression of the disease.

With regard to AICD, it can be produced from the non amyloidogenic pathway, but different studies report that this fragment preferentially derives from the β-secretase produced CTF in the amyloidogenic pathway (Goodger et al. 2009). AICD has transactivation properties within the nucleus, and activates the expression of specific genes involved in cellular pathways, whose pathogenetic role in AD is well recognized. In our study, we demonstrate that HSV-1 induced AICD formation and its nuclear localization. The subcellular trafficking of AICD foresees the binding of this fragment to the adaptor protein Fe65 and the translocation to the nucleus (Kimberly et al. 2001). Within the nuclei, the complex AICD-Fe65 interacts with the histone acetylase Tip60 in order to form the AFT-complex, whose precise role is still unknown (von Rotz et al. 2004). It is possible to speculate that AICD spots in the nuclei reflect the formation of these AFT-complexes and, in turn, an increase in the rate of gene transcription (von Rotz et al. 2004). Accordingly, we found that AICD was physically present at the promoter region of *nep* and *gsk3β* genes. In particular, we

found that, after HSV-1 infection, newly produced AICD promoted the transcription of *nep* gene, but such an effect was transient as, later in infection, *nep* mRNA and protein, as well as the enzymatic activity were reduced. This result is in agreement with data obtained by others in different experimental models as transgenic mice and brain slices (Zhou et al. 2013; Caccamo et al. 2005), and may act by boosting Aβ deposition. In fact, NEP is an integral membrane protein that is predominantly localized at synapses and along the axons (Fukami et al. 2002), and it is considered the major Aβ-degrading enzyme, since it clears both Aβ monomers and oligomers (Kanemitsu et al. 2003). Several evidence support its important role in Aβ clearance: *nep* knock-out mice show the build-up of Aβ levels within the brain (Iwata et al. 2001), whereas over-expression of NEP correlates with reduced Aβ content and plaque load (El-Amouri et al. 2008). In AD brains, there is an alteration in protein expression levels, specifically in the hippocampus or cortex, but not in the cerebellum, which is less sensitive to AD pathology (Caccamo et al. 2005). A recent paper demonstrates that NEP protein levels are modulated in brains of APP/PS1 transgenic mice (Zhou et al. 2013). In particular, NEP levels in the mice cortex are increased at 3 months, followed by a reduction at 6 month of age, and this pattern resembles the findings observed in AD patients. Accordingly, the decrease in both NEP protein level and enzymatic activity observed in our study might be due to Aβ accumulation we have already demonstrated in HSV-1-infected neuronal cells (Piacentini et al. 2011; De Chiara et al. 2010). Furthermore, previous data revealed that NEP is modified by oxidative conditions, such as those produced by lipid peroxidation, which reduce NEP catalytic activity in AD (Wang et al.
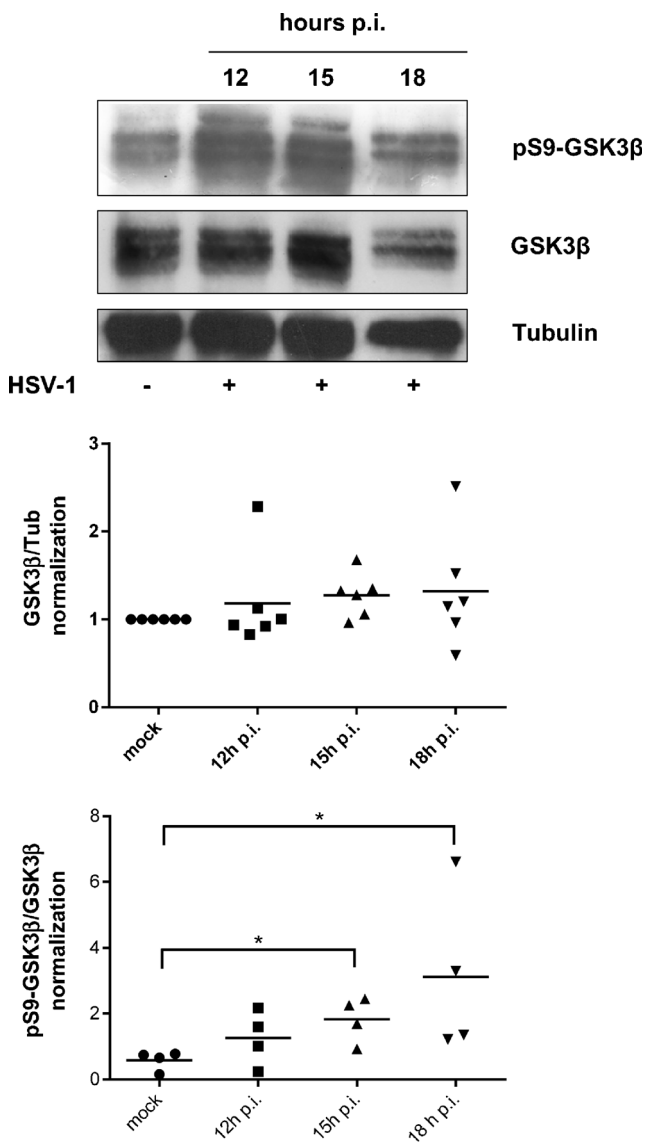
Fig. 5 HSV-1 infection does not significantly alter GSK3β protein expression levels, but modulates its enzymatic activity. Representative blot of rat cortical neuron lysates harvested at the indicated times post HSV-1- or mock-infection. Blot was firstly probed with anti-phospho-Ser9-GSK3β antibody, then stripped and re-probed with anti-total-GSK3β or anti-Tubulin antibodies. Densitometric analysis of total GSK3β or phospho-Ser9-GSK3β levels from six and four different experiments, respectively, are shown in the graphs below the western blot, *$p < 0.05$ HSV-1 vs mock

2009). It is known that HSV-1 induces intracellular oxidative stress (Kavouras et al. 2007; Palamara et al. 1995), so we may speculate that, during the infection, the increase in the level of soluble lipid peroxidation products may concur to NEP modification and reduction of its catalytic ability, with consequent reduced capacity to clear Aβ.

GSK3β is a serine/threonine kinase, which is involved in signaling processes in the brain and promotes key events in neuronal dysfunction, such as the hyperphosphorylation of tau and the increased Aβ production (Hooper et al. 2008). Some

authors demonstrated that AICD promotes the gene transcription of GSK3β (Chang et al. 2006). In our experimental conditions, although AICD was physically at the promoter region of *gsk3*β gene, the expression of GSK3β at the protein level was stable along the progression of HSV-1 infection, suggesting that this gene undergoes a different transcriptional control at least during viral infection. GSK3β activation depends on the phosphorylation status of two specific sites: serine 9 (Ser9), whose phosphorylation causes the inactivation of the protein, and tyrosine 216 (Tyr216) that, when phosphorylated, enhances its kinase activity. In resting cells, GSK3β shows high activity, but different signals can induce its rapid deactivation through complex mechanisms (Medina and Wandosell 2011). Interestingly, dysregulation of GSK3β activity has been found in AD, and recent studies reported abnormal activation of this kinase in AD compared to healthy brains (Leroy et al. 2007). In our experimental model, the enzyme was phosphorylated in Ser9 only at later stages of the infection, suggesting that GSK3β is active earlier, and its late inactivation might be due to a feedback mechanism related to the increased levels of phosphorylated substrates during infection. Recent findings from Naghavi et al. (2013) demonstrate that in human fibroblasts, the herpetic US3 kinase phosphorylates GSK3β at Ser9, which causes its inactivation and thus promotes virus spread through cellular microtubule network. It is possible to hypothesize that a similar mechanism may be induced by the virus in neurons as well. Other studies indicated that the inhibition of GSK3β activity is mainly responsible of lysosomal acidification, which restores lysosomal activity altered by different conditions, such as overexpression of APP (Avrahami et al. 2013). Since a block of the endosomal or autophagic pathways, which remove undegraded material through a flux toward lysosomes, have been recognized as one of the factor promoting the accumulation of Aβ aggregates (Yang et al. 2011), it is possible to speculate that the GSK3β inactivation in the late step of viral infection may also be a cell strategy to restore lysosomal functionality and boost clearance of Aβ produced by HSV-1 induced APP processing.

In conclusion, overall, these data demonstrate that HSV-1 infection in neurons leads to the production and nuclear translocation of APP-derived fragments that are able to bind the promoter region of two specific genes, NEP and GSK3β, which are known to have a pivotal role in the amyloid cascade. We know that our results have been obtained in an acute model of infection that could be very different from a "milder" infection of the brain that periodically follows viral reactivation. It is possible to speculate that HSV-1-induced neurotoxic effects, when repeated several time during the life, may lead to the accumulation of "toxic bricks" in neurons, contributing to

AD pathogenesis simultaneously and independently from other risk factors.

Conflict of interest All authors, Livia Civitelli, Maria Elena Marcocci, Ignacio Celestino, Roberto Piacentini, Enrico Garaci, Claudio Grassi, Giovanna De Chiara and Anna Teresa Palamara, declare that they have no conflict of interest.

References

Avrahami L, Farfara D, Shaham-Kol M, Vassar R, Frenkel D, Eldar-Finkelman H (2013) Inhibition of glycogen synthase kinase-3 ameliorates β-amyloid pathology and restores lysosomal acidification and mammalian target of rapamycin activity in the Alzheimer disease mouse model: in vivo and in vitro studies. J Biol Chem 288: 1295–1306

Belyaev ND, Nalivaeva NN, Makova NZ, Turner AJ (2009) Neprilysin gene expression requires binding of the amyloid precursor protein intracellular domain to its promoter: implications for Alzheimer disease. EMBO Rep 10:94–100. doi:10.1038/embor.2008.222

Caccamo A, Oddo S, Sugarman MC, Akbari Y, LaFerla FM (2005) Age- and region-dependent alterations in Abeta-degrading enzymes: implications for Abeta-induced disorders. Neurobiol Aging 26:645–654

Cao X, Südhof TC (2001) A transcriptionally [correction of transcriptively] active complex of APP with Fe65 and histone acetyltransferase Tip60. Science 293:115–120

Chang KA, Kim HS, Ha TY, Ha JW, Shin KY, Jeong YH, Lee JP, Park CH, Kim S, Baik TK, Suh YH (2006) Phosphorylation of amyloid precursor protein (APP) at Thr668 regulates the nuclear translocation of the APP intracellular domain and induces neurodegeneration. Mol Cell Biol 26:4327–4338

De Chiara G, Marcocci ME, Civitelli L, Argnani R, Piacentini R, Ripoli C, Manservigi R, Grassi C, Garaci E, Palamara AT (2010) APP processing induced by herpes simplex virus type 1 (HSV-1) yields several APP fragments in human and rat neuronal cells. PLoS One 5, e13989. doi:10.1371/journal.pone.0013989

De Chiara G, Marcocci ME, Sgarbanti R, Civitelli L, Ripoli C, Piacentini R, Garaci E, Grassi C, Palamara AT (2012) Infectious agents and neurodegeneration. Mol Neurobiol 46:614–638

Dobson CB, Itzhaki RF (1999) Herpes simplex virus type 1 and Alzheimer's disease. Neurobiol Aging 20:457–465

El-Amouri SS, Zhu H, Yu J, Marr R, Verma IM, Kindy MS (2008) Neprilysin: an enzyme candidate to slow the progression of Alzheimer's disease. Am J Pathol 172:1342–1354

Fukami S, Watanabe K, Iwata N, Haraoka J, Lu B, Gerard NP, Gerard C, Fraser P, Westaway D, St George-Hyslop P, Saido TC (2002) Abeta-degrading endopeptidase, neprilysin, in mouse brain: synaptic and axonal localization inversely correlating with Abeta pathology. Neurosci Res 43:39–56

Goodger ZV, Rajendran L, Trutzel A, Kohli BM, Nitsch RM, Konietzko U (2009) Nuclear signaling by the APP intracellular domain occurs predominantly through the amyloidogenic processing pathway. J Cell Sci 122:3703–3714

Haass C, Kaether C, Thinakaran G, Sisodia S (2012) Trafficking and proteolytic processing of APP. Cold Spring Harb Perspect Med 5: a006270

Hooper C, Killick R, Lovestone S (2008) The GSK3 hypothesis of Alzheimer's disease. J Neurochem 104:1433–1439

Iwata N, Tsubuki S, Takaki Y, Shirotani K, Lu B, Gerard NP, Gerard C, Hama E, Lee HJ, Saido TC (2001) Metabolic regulation of brain Abeta by neprilysin. Science 292:1550–1552

Kanemitsu H, Tomiyama T, Mori H (2003) Human neprilysin is capable of degrading amyloid beta peptide not only in the monomeric form but also the pathological oligomeric form. Neurosci Lett 350:113–116

Kavouras JH, Prandovszky E, Valyi-Nagy K, Kovacs SK, Tiwari V, Kovacs M, Shukla D, Valyi-Nagy T (2007) Herpes simplex virus type 1 infection induces oxidative stress and the release of bioactive lipid peroxidation by-products in mouse P19N neural cell cultures. J Neurovirol 13:416–425

Killington RA, Powell KL (1991) Growth, assay and purification of herpesviruses. In: Mahy BWJ (ed), IRL Press Virology: a pratical approach, Oxford. pp. 212–213

Kimberly WT, Zheng JB, Guénette SY, Selkoe DJ (2001) The intracellular domain of the β-amyloid precursor protein is stabilized by Fe65 and translocates to the nucleus in a notch-like manner. J Biol Chem 276:40288–40292

Lefranc-Jullien S, Sunyach C, Checler F (2006) APPε, the ε-secretase-derived N-terminal product of the β-amyloid precursor protein, behaves as a type I protein and undergoes α-, β-, and γ-secretase cleavages. J Neurochem 97:807–817

Lerchundi R, Neira R, Valdivia S, Vio K, Concha MI, Zambrano A, Otth C (2011) Tau cleavage at D421 by caspase-3 is induced in neurons and astrocytes infected with herpes simplex virus type 1. J Alzheimers Dis 23:513–520

Leroy K, Yilmaz Z, Brion JP (2007) Increased level of active GSK-3beta in Alzheimer's disease and accumulation in argyrophilic grains and in neurones at different stages of neurofibrillary degeneration. Neuropathol Appl Neurobiol 33:43–55

Lesné S, Koh MT, Kotilinek L, Kayed R, Glabe CG, Yang A, Gallagher M, Ashe KH (2006) A specific amyloid-beta protein assembly in the brain impairs memory. Nature 440:352–357

Li C, Booze RM, Hersh LB (1995) Tissue-specific expression of rat neutral endopeptidase (neprilysin) mRNAs. J Biol Chem 270: 5723–5728

Masters CL, Selkoe DJ (2012) Biochemistry of amyloid β-protein and amyloid deposits in Alzheimer disease. Cold Spring Harb Perspect Med 2:a006262

Medina M, Wandosell F (2011) Deconstructing GSK-3: the fine regulation of its activity. Int J Alzheimers Dis 2011:479249

Mori I, Kimura Y, Naiki H, Matsubara R, Takeuchi T et al (2004) Reactivation of HSV-1 in the brain of patients with familial Alzheimer's disease. J Med Virol 73:605–611

Naghavi MH, Gundersen GG, Walsh D (2013) Plus-end tracking proteins, CLASPs, and a viral Akt mimic regulate herpesvirus-induced stable microtubule formation and virus spread. Proc Natl Acad Sci U S A 110:18268–18273. doi:10.1073/pnas.1310760110

Nixon RA (2007) Autophagy, amyloidogenesis and Alzheimer disease. J Cell Sci 120:4081–4091

Palamara AT, Perno CF, Ciriolo MR, Dini L, Balestra E, D'Agostini C, Di Francesco P, Favalli C, Rotilio G, Garaci E (1995) Evidence for antiviral activity of glutathione: in vitro inhibition of herpes simplex virus type 1 replication. Antiviral Res 27:237–353

Piacentini R, Civitelli L, Ripoli C, Marcocci ME, De Chiara G, Garaci E, Azzena GB, Palamara AT, Grassi C (2011) HSV-1 promotes Ca2+-mediated APP phosphorylation and Aβ accumulation in rat cortical neurons. Neurobiol Aging 32:2323.e13–2323.e26. doi:10.1016/j.neurobiolaging.2010.06.009

Piacentini R, De Chiara G, Li Puma DD, Ripoli C, Marcocci ME, Garaci E, Palamara AT, Grassi C (2014) HSV-1 and Alzheimer's disease: more than a hypothesis. Front Pharmacol 5:97

Santana S, Recuero M, Bullido MJ, Valdivieso F, Aldudo J (2012) Herpes simplex virus type I induces the accumulation of intracellular β-amyloid in autophagic compartments and the inhibition of the non-amyloidogenic pathway in human neuroblastoma cells. Neurobiol Aging 33:430.e19–430.e33

Sergeant N, David JP, Champain D, Ghestem A, Wattez A, Delacourte A (2002) Progressive decrease of amyloid precursor protein carboxy terminal fragments (APP-CTFs), associated with tau pathology stages, in Alzheimer's disease. J Neurochem 81:663–672

Shipley SJ, Parkin ET, Itzhaki RF, Dobson CB (2005) Herpes simplex virus interferes with amyloid precursor protein processing. BMC Microbiol 5:48

Słomnicki LP, Leśniak W (2008) A putative role of the amyloid precursor protein intracellular domain (AICD) in transcription. Acta Neurobiol Exp 68:219–228

von Rotz RC, Kohli BM, Bosset J, Meier M, Suzuki T, Nitsch RM, Konietzko U (2004) The APP intracellular domain forms nuclear multiprotein complexes and regulates the transcription of its own precursor. J Cell Sci 117:4435–4448

Wang R, Wang S, Malter JS, Wang DS (2009) Effects of HNE-modification induced by Aβ on neprilysin expression and activity in SH-SY5Y cells. J Neurochem 108:1072–1082

Wang S, Wang R, Chen L, Bennett DA, Dickson DW, Wang DS (2010) Expression and functional profiling of neprilysin, insulin-degrading enzyme, and endothelin-converting enzyme in prospectively studied elderly and Alzheimer's brain. J Neurochem 115:47–57

Weinmann AS, Farnham PJ (2002) Identification of unknown target genes of human transcription factors using chromatin immunoprecipitation. Methods 26:37e47

Wozniak MA, Itzhaki RF, Shipley SJ, Dobson CB (2007) Herpes simplex virus infection causes cellular beta-amyloid accumulation and secretase upregulation. Neurosci Lett 429:95–100

Wozniak MA, Frost AL, Itzhaki RF (2009) Alzheimer's disease-specific tau phosphorylation is induced by herpes simplex virus type 1. J Alzheimers Dis 16:341–350. doi:10.3233/JAD-2009-0963

Xu F, Sternberg M, Kottiri B, McQuillan G, Lee F, Nahmias AJ, Berman SM, Markowitz LE (2006) Trends in herpes simplex virus type 1 and type 2 seroprevalence in the United States. JAMA 296:964–973

Yang DS, Stavrides P, Mohan PS, Kaushik S, Kumar A, Ohno M, Schmidt SD, Wesson D, Bandyopadhyay U, Jiang Y, Pawlik M, Peterhoff CM, Yang AJ, Wilson DA, St George-Hyslop P, Westaway D, Mathews PM, Levy E, Cuervo AM, Nixon RA (2011) Reversal of autophagy dysfunction in the TgCRND8 mouse model of Alzheimer's disease ameliorates amyloid pathologies and memory deficits. Brain 134:258–277

Zambrano A, Solis L, Salvadores N, Cortés M, Lerchundi R, Otth C (2008) Neuronal cytoskeletal dynamic modification and neurodegeneration induced by infection with herpes simplex virus type 1. J Alzheimers Dis 14:259–269

Zhang YW, Thompson R, Zhang H, Xu H (2011) APP processing in Alzheimer's disease. Mol Brain 4:3

Zhou L, Wei C, Huang W, Bennett DA, Dickson DW, Wang R, Wang D (2013) Distinct subcellular patterns of neprilysin protein and activity in the brains of Alzheimer's disease patients, transgenic mice and cultured human neuronal cells. Am J Transl Res 5:608–621